Dalton Transactions

PAPER

View Article Online
View Journal | View Issue

Cite this: *Dalton Trans.*, 2017, **46**, 11890

Magneto-structural correlations in dirhenium(IV) complexes possessing magnetic pathways with even or odd numbers of atoms†

Anders H. Pedersen, [a] Miguel Julve, [b] José Martínez-Lillo, *[b] Joan Cano *[b] and Euan K. Brechin *[a]

Received 18th July 2017,
Accepted 14th August 2017

DOI: 10.1039/c7dt02612a

rsc.li/dalton

The employment of pyrazine (pyz), pyrimidine (pym) and *s*-triazine (triz) ligands in Re^{IV} chemistry leads to the isolation of a family of complexes of general formula $(NBu_4)_2[(ReX_5)_2(\mu\text{-}L)]$ (L = pyz, X = Cl (**1**) or Br (**2**); L = pym, X = Br (**3**); L = triz, X = Br (**4**)). **1–4** are dinuclear compounds where two pentahalorhenium(IV) fragments are connected by bidentate pyz, pym and triz ligands. Variable-temperature magnetic measurements, in combination with detailed theoretical studies, uncover the underlying magneto-structural correlation whereby the nature of the exchange between the metal ions is dictated by the number of intervening atoms. That is, the spin-polarization mechanism present dictates that odd and even numbers of atoms favour ferromagnetic (F) and antiferromagnetic (AF) exchange interactions, respectively. Hence, while the pyz ligand in **1** and **2** mediates AF coupling, the pym and triz ligands in **3** and **4** promote F interactions.

Introduction

In 1963 McConnell proposed a mechanism to describe the magnetic exchange between radicals in aromatic organic molecules.[1] Antiferromagnetic and ferromagnetic interactions, with singlet and triplet ground spin states, were favoured when the magnetic pathway was made up of even or odd numbers of atoms, respectively. Such a mechanism therefore dictated that the more stable spin configuration described an alternation of spin densities on adjacent atoms in the π-pathway through dynamic spin polarization, *i.e.* an 'up–down–up–down' arrangement. This proposal created new research avenues in the field of molecular magnetism, attracting great interest over several decades.[2–7] However, doubts existed about its application to inorganic systems where the spin carriers were metal ions. For example, a dinuclear Ti^{III} complex synthesized in the 1970s unexpectedly displayed moderate ferromagnetic exchange as a consequence of a spin polarization mechanism of exchange. Although this was the very first example of an inorganic system exhibiting such behaviour, the result was largely ignored and remained unexploited for some time.[8,9] Two decades later, the first magnetic systems with an operative McConnell mechanism containing paramagnetic metal ions were reported; these were "dinuclear" systems where one paramagnetic centre was a metal ion and the other an organic radical.[10–12] In the early 1990s, the first purely inorganic systems based on Mo^{III} and Co^{II} ions were reported.[13–20] In the latter case, the nature of the magnetic coupling was nicely tuned (ferromagnetic *vs.* antiferromagnetic) using diazine type ligands that provided π-exchange pathways with even or odd numbers of atoms. To this point all known inorganic systems were based on metal ions possessing magnetic t_{2g} orbitals interacting with a π-pathway. Metal complexes with magnetic e_g orbitals were not considered good candidates as they were assumed to promote spin delocalization. However, in 2001, this position was challenged when strong spin polarization between d^9 Cu^{II} ions was observed,[21] opening the door toward further research focussing on the study of magnetic communication across long intermetallic distances, and the application of these concepts in, for example, spintronics.[22–26] In this paper, we have adapted this approach by employing pyrazine (pyz), pyrimidine (pym) and *s*-triazine (triz) ligands to examine the nature and magnitude of magnetic exchange between Re^{IV} ions ($5d^3$ electronic configuration), leading to the first magneto-structural correlation of dinuclear $[Re_2^{IV}]$ molecules of general formula $(NBu_4)_2[(ReX_5)_2(\mu\text{-}L)]$ (L = pyz, X = Cl (**1**) or Br (**2**); L = pym, X = Br (**3**); L = triz, X = Br (**4**)).

[a]*EaStCHEM School of Chemistry, The University of Edinburgh, David Brewster Road, EH9 3FJ Edinburgh, UK. E-mail: E.Brechin@ed.ac.uk*
[b]*Departament de Química Inorgànica/Instituto de Ciencia Molecular (ICMol), Universitat de València, C/Catedrático José Beltrán 2, Paterna, València, Spain. E-mail: joan.cano@uv.es, F.Jose.Martinez@uv.es*

†Electronic supplementary information (ESI) available. CCDC 1557650–1557653. For ESI and crystallographic data in CIF or other electronic format see DOI: 10.1039/c7dt02612a

Experimental section

Materials and methods

All chemicals were used as received. Syntheses were carried out under aerobic conditions. $(NBu_4)_2[ReCl_6]$ and $(NBu_4)_2[ReBr_6]$ (NBu_4^+ = tetra-*n*-butylammonium cation) were prepared as described previously.[27,28] Crystals of **1–4** were collected and left open to air for use in further analysis. Elemental analyses (C, H, N) were performed by MEDAC Ltd. Direct current (dc) magnetic susceptibility measurements were performed on a Quantum Design MPMS-XL SQUID magnetometer equipped with a 7 T dc magnet in the temperature range 300–2.0 K. Diamagnetic corrections were applied using Pascal's constants.[29]

Synthesis of $(NBu_4)_2[(ReCl_5)_2(\mu\text{-pyz})]$ (1)

$(NBu_4)_2[ReCl_6]$ (0.10 mmol, 88.0 mg) and pyrazine (0.20 mmol, 16.0 mg) in 4.5 cm^3 of glacial acetic acid were stirred at 100 °C for 8 hours, after which a dark red solid was collected by filtration. The solid was dissolved in dichloromethane (DCM) and layered with glacial acetic acid. Red crystals of **1** suitable for X-ray diffraction were collected after 3 days (yield *ca.* 17%). Elemental analysis (%) calculated (found) for $C_{36}H_{76}Cl_{10}N_4Re_2$ (**1**): C, 33.5 (33.5); H, 5.9 (5.9); N, 4.3 (4.2).

Synthesis of $(NBu_4)_2[(ReBr_5)_2(\mu\text{-pyz})]$ (2)

$(NBu_4)_2[ReBr_6]$ (0.10 mmol, 115.0 mg) and pyrazine (0.20 mmol, 16.0 mg) in 4.5 cm^3 of glacial acetic acid were heated at 80 °C for 4 hours with stirring, and the resulting red solid was collected by filtration. It was dissolved in DCM and diffused with diethyl ether vapour. Brown single crystals of **2** were grown after 2 days (yield *ca.* 31%). Elemental analysis (%) calculated (found) for $C_{36}H_{76}Br_{10}N_4Re_2$ (**2**): C, 24.9 (25.0); H, 4.4 (4.3); N, 3.2 (3.0).

Synthesis of $(NBu_4)_2[(ReBr_5)_2(\mu\text{-pym})]$ (3)

$(NBu_4)_2[ReBr_6]$ (0.10 mmol, 115.0 mg) and pyrimidine (0.20 mmol, 16 μl) were mixed in 4.5 cm^3 of glacial acetic acid. The solution was stirred at 80 °C for 2 hours and the resulting precipitate was collected by filtration. It was dissolved in DCM and layered with isopropanol. X-ray quality crystals of **3** were collected after 3 days (yield *ca.* 13%). Elemental analysis (%) calculated (found) for $C_{36}H_{76}Br_{10}N_4Re_2$ (**3**): C, 24.9 (25.0); H, 4.4 (4.3); N, 3.2 (3.1).

Synthesis of $(NBu_4)_2[(ReBr_5)_2(\mu\text{-triz})]$ (4)

$(NBu_4)_2[ReBr_6]$ (0.10 mmol, 115.0 mg) and *s*-triazine (0.20 mmol, 16.2 mg) in 4.5 cm^3 of glacial acetic acid were stirred at 75 °C for 4 hours. The orange precipitate formed was collected by filtration, dissolved in DCM and layered with glacial acetic acid. After 2 days, large orange crystals suitable for X-ray diffraction had formed (yield *ca.* 19%). Elemental analysis (%) calculated (found) for $C_{35}H_{75}Br_{10}N_5Re_2$ (**4**): C, 24.2 (24.3); H, 4.4 (4.3); N, 4 (3.8).

Crystallography

Data were obtained on Rigaku Oxford Diffraction SuperNova (**1**, **2**, **4**) and Rigaku Oxford Diffraction XCalibur (**3**) X-ray diffractometers using Mo-K_α radiation. Structures were solved with olex2.solve (**2**, **3**)[30] or ShelXS (**1**, **4**)[31] and refined by full-matrix least-squares on *F*-squared using ShelXL, interfaced through Olex2.[32] All non-hydrogen atoms were refined anisotropically. Hydrogen atom parameters were constrained. For full details see Table S1.† CCDC 1557650–1557653.†

Computational details

In order to estimate the nature and magnitude of the intramolecular magnetic exchange interactions in **1–4**, calculations were performed with the Gaussian09 package using the CAM-B3LYP functional (a long range corrected version of B3LYP) and the quadratic convergence approach.[33–37] Double-ζ and Los Alamos effective core potentials, as proposed by Hay and Wadt, were used for Re^{IV}, Cl^- and Br^- ions.[38–40] Ahlrichs double-ζ basis set was used for the remaining atoms.[41] Two-electron integrals and their derivatives were computed from Douglas–Kroll–Hess (DKH) 2nd order scalar relativistic calculations.[42,43] An approach based on the use of broken-symmetry (BS) functions built from localized orbitals was used to evaluate the energies of several spin states.[44] The BS functions, which provide positive or negative spin densities on the paramagnetic centres, were obtained from the guess functions generated with the fragment tool implemented in Gaussian09. Intermolecular magnetic couplings for the shortest contacts were calculated from the experimental structures. Parameters corresponding to the acetonitrile solvent were included to simulate the electronic effects of the surrounding molecules.[45] Calculations of the zero-field splitting (zfs) parameters were performed with version 3.0 of the ORCA program.[46] The TZVP basis set proposed by Ahlrichs, and tight SCF criteria were used in all cases.[41] Relativistic effects for the Re^{IV} ions were introduced from a zero-order regular approximation (ZORA).[47] For complete active space (CAS) calculations, this auxiliary basis set was replaced by TZV/C.[48–50] Experimental geometries of **1** and **2** were used in the theoretical calculations. The zfs parameters were evaluated from Complete Active Space (CAS) and N-Electron Valence State Perturbation Theory (NEVPT2) calculations and an approach based on a 2^{nd} order Hamiltonian for the spin–orbit coupling. This zfs calculation included contributions from ten quartet and twenty doublet states generated from electron promotion between d orbitals, which corresponds to the full active space built from only the five d orbitals of the Re^{IV} ion.[51–53]

Results and discussion

Description of the crystal structures of 1–4

Complex **1** crystallises in the monoclinic space group $P2_1/c$ and its structure consists of tetrabutylammonium cations and the dinuclear $[(ReCl_5)_2(\mu\text{-pyz})]^{2-}$ complex anion (Fig. 1a). Each Re^{IV}

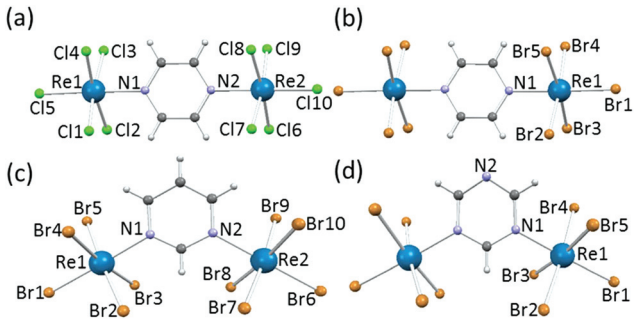

Fig. 1 The structures of the anions of **1–4** (a–d). Colour code: Re, cyan; Br, brown; Cl, green; C, grey; N, blue; H, white.

ion is six-coordinate with five chloride ions and a nitrogen atom from the pyrazine ligand building a slightly distorted octahedral geometry. The Re–Cl bond lengths vary in the range 2.3006(8)–2.3552(8) Å, and the Re(1)–N(1) and Re(2)–N(2) bond lengths are 2.180(2) and 2.175(2) Å, respectively (Table S2†). The intramolecular Re···Re separation is 7.1354(3) Å, with the pyrazine ligand twisted out of the Re_2Cl_6 plane by approximately 45°. The Re^{IV} ions are positioned out of the equatorial Cl_4 plane away from the pyrazine ligand by 0.1186(4) Å for Re(1) and 0.1207(4) Å for Re(2). The structural parameters of the Re^{IV} ions are similar to those published for the $[ReCl_5(pyz)]^-$ monomer,[54] and the C–C and C–N bond lengths of the pyrazine ligand agree with previously published results.[55,56] Each $[(ReCl_5)_2\mu\text{-pyz}]^{2-}$ unit is well isolated from adjacent anions by the bulky NBu_4^+ cations, as shown in the crystal packing (Fig. S1†). The organic cations pack around the complex anions through numerous C–H···Cl type interactions, with the shortest intermolecular Cl···Cl and Re···Re distances being 4.6976(11) and 8.3503(3) Å, respectively (Table S3†).

Compound **2** crystallises in the monoclinic space group $P2_1/n$ (Table S1†). The asymmetric unit contains half of the $[(ReBr_5)_2\mu\text{-pyz}]^{2-}$ complex anion and one NBu_4^+ cation, due to the presence of an inversion centre which is positioned at the centroid of the pyrazine ligand (Fig. 1b). Each Re^{IV} ion is coordinated to five bromide ions and a nitrogen atom from the pyrazine ligand. The Re–Br bond lengths range from 2.4489(6) to 2.4953(6) Å, with the Re–N bond being 2.196(4) Å (Table S2†). The pyrazine moiety is disordered over two positions with the plane of the ligand twisted with respect to the Re_2Br_6 plane at inter-plane angles of 40° and 44°. The Re^{IV} ion is displaced out of the equatorial Br_4 plane away from the pyrazine ligand by 0.1148(4) Å. The geometrical parameters for the Re^{IV} ion agree with those in the previously published species $NBu_4[ReBr_5(Hpyzc)]$ (Hpyzc = 2-pyrazinecarboxylic acid).[57] The intradimer Re···Re separation is 7.1723(4) Å. The NBu_4^+ cations in the crystal lattice pack around the complex anions, connected *via* numerous C–H···Br type interactions. Short Br···Br contacts occur between the complex anions, the shortest distance being 3.5202(9) Å [Br(2)···Br(2)′] creating a 1D network of complex anions interacting in an end-to-end fashion along the crystallographic *a*-axis (Fig. S2†). This causes the shortest intermolecular Re···Re distance to be 8.4862(5) Å.

Complex **3** crystallises in the monoclinic space group $P2_1$ with the asymmetric unit containing two $(NBu_4)_2[(ReBr_5)_2(\mu\text{-pym})]$ complexes. The two $[(ReBr_5)_2(\mu\text{-pym})]^{2-}$ anions display nearly identical coordination geometries, with the first coordination sphere of the Re^{IV} ions similar to that described for **2** (Fig. 1c and Table S2†). The values of the C–C and C–N bond lengths of the bridging pyrimidine ligand agree with those of previously published structures containing this ligand.[58] The two Re^{IV} ions are disposed at an angle of approximately 118° with respect to the centre of the pyrimidine moiety, with the organic ligand positioned equidistant between the two perpendicular $[ReCl_4]$ planes. The intradimer Re···Re distance is *ca.* 6.1 Å, with the shortest intramolecular Br···Br contact being 4.006(2) Å (Br(12)···Br(18)) (Table S3†). Numerous C–H···Br type interactions are present between the complex anions and organic cations in the crystal lattice, causing each $[(ReBr_5)_2(\mu\text{-pym})]^{2-}$ moiety to be well isolated from it's neighbours – the shortest intermolecular Br···Br contact being 4.707(2) Å (Fig. S3†).

Complex **4** crystallises in the monoclinic space group $I2/a$. The asymmetric unit contains one NBu_4^+ cation and half a $[(ReBr_5)_2(\mu\text{-triz})]^{2-}$ anion, due to a two-fold rotation axis intersecting the C(2) and N(2) atoms on the *s*-triazine ligand. The Re^{IV} ion sits in a coordination sphere similar to the one described for complex **2** (Fig. 1d and Table S2†). The triazine molecule contains C–C and C–N bond lengths which correlate well with previously published results describing this ligand bridging two metal ions.[59] In the $[(ReBr_5)_2(\mu\text{-triz})]^{2-}$ unit the two Re^{IV} ions are placed at an angle of 121.91(4)° with respect to the triazine centroid, at a distance of 6.2390(4) Å. The shortest intramolecular Br···Br contact is 4.5249(4) Å [Br(2)···Br(3)′] (Table S3†). The organic ligand is again positioned equidistant between the two approximately perpendicular $[ReBr_4]$ planes. The complex anions in the crystal packing interact through short Br···Br interactions [Br(5)···Br(5)′ = 3.4304(4) Å] between neighbouring $[(ReBr_5)_2(\mu\text{-triz})]^{2-}$ units (Fig. S4†). The shortest intermolecular Re···Re distance is 8.4090(3) Å.

Magnetic behaviour of 1–4

The magnetic behaviour of complexes **1–4** in the form of $\chi_M T$ *vs.* *T* plots is shown in Fig. 2–5 (χ_M being the molar magnetic susceptibility per two Re^{IV} ions). The $\chi_M T$ values at room temperature (2.68–3.36 $cm^3\ mol^{-1}\ K$) are close to that expected for two $S = 3/2$ spin centres with $g = 1.7–1.9$. On cooling, the value of $\chi_M T$ continuously decreases for **1** and **2**, approaching zero at the lowest temperatures measured, accompanied by the appearance of a maximum in χ_M at ~45 K. This is suggestive of the presence of antiferromagnetic exchange between the metal ions, in concert with the large zero-field splitting [defined by the axial (D) and rhombic (E) components] expected for a Re^{IV} ion (Fig. 2 and 3). In contrast, the $\chi_M T$ values for complexes **3** and **4** (Fig. 4 and 5) increase slowly with decreasing temperature until approximately 30 K, before collapsing at lower temp-

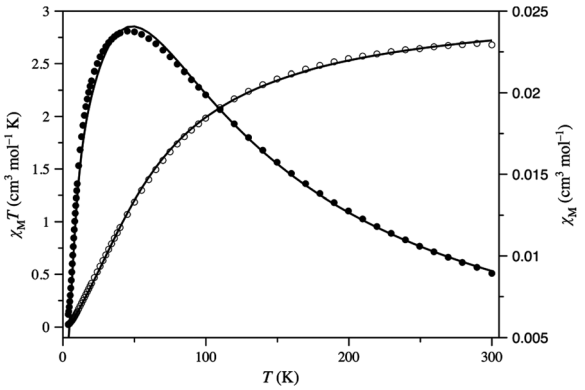

Fig. 2 Thermal dependence of $\chi_M T$ (○) and χ_M (●) under an applied dc field of 0.1 T for **1**. The solid line is the best-fit curve (see the text).

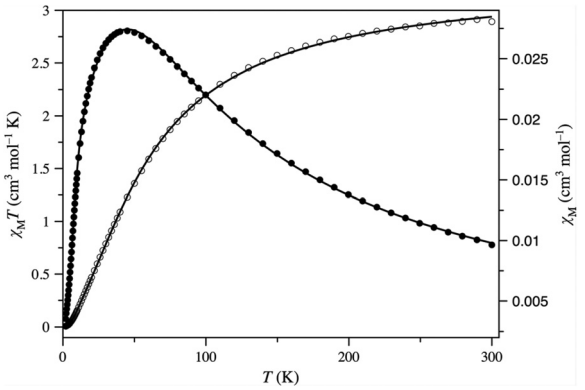

Fig. 3 Thermal dependence of $\chi_M T$ (○) and χ_M (●) under an applied dc field of 0.1 T for **2**. The solid line is the best-fit curve (see the text).

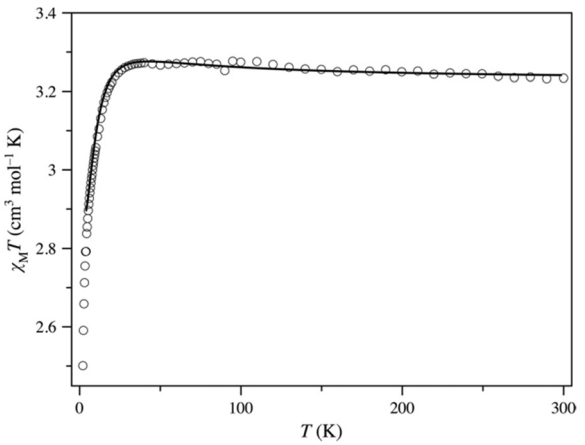

Fig. 4 Thermal dependence of $\chi_M T$ (○) under an applied dc field of 0.1 T for **3**. The solid line is the best-fit curve (see the text).

eratures. The behaviour in the high temperature region is indicative of ferromagnetic exchange between the Re^{IV} ions and that at lower temperatures is potentially ascribed to zfs

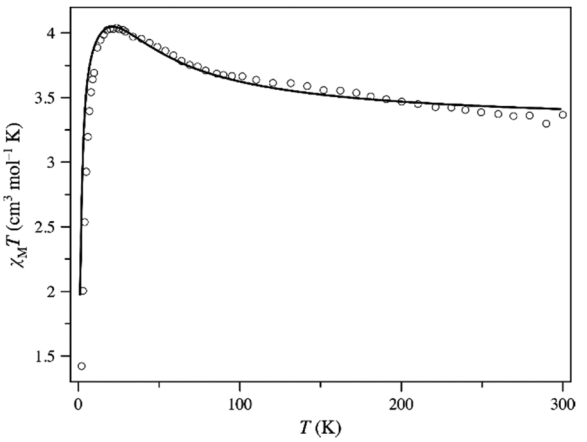

Fig. 5 Thermal dependence of $\chi_M T$ (○) under an applied dc field of 0.1 T for **4**. The solid line is the best-fit curve (see the text).

effects and/or antiferromagnetic intermolecular exchange interactions.

Simulations based on a simple model can be used to help in the deconvolution of all the potential contributions to the magnetic data, providing a qualitative initial view of how different physical phenomena contribute. These simulations, through spin-Hamiltonian (1) and shown in Fig. 6, are based on two $S = 3/2$ ions and include both exchange (J) and axial zfs (D) parameters possessing a variety of signs and magnitudes. The local zfs tensors have been considered collinear in all cases. In this model, the sign of D has no effect on the thermal dependence of the magnetic susceptibility in the lack of magnetic exchange, and it is almost negligible in the case of antiferromagnetic exchange. When J is positive and D is non-zero a decrease in the $\chi_M T$ product is observed at low temperatures for both positive and negative values of D. Given the large intermolecular distances observed in the extended structures of **3** and **4**, the decrease in $\chi_M T$ below 30 K for both is initially attributed to the zfs effects (*vide infra*), but the simulations cannot distinguish between local positive and negative D values (for $T > 5$ K).

$$\hat{H} = \sum_{i=1}^{2} g_{Re} B \beta \hat{S}_i + D[(\hat{S}_i^z)^2 - S_i(S_i+1)/3] + E[(\hat{S}_i^x)^2 - (\hat{S}_i^y)^2] - J\hat{S}_1\hat{S}_2 \quad (1)$$

In certain Re^{IV} complexes, non-zero/non-negligible intermolecular magnetic exchange interactions can be observed, because of the presence of large spin densities on the coordinated ligands, originating from the π-spin delocalization from the t_{2g} magnetic orbitals. This is particularly evident when there are chloride or bromide anions as ligands.[60] These interactions can be avoided by isolating the metal complexes from each other through the use of bulky counter ions, as is done here. In order to check that intermolecular interactions do not play a prominent role in the low temperature magnetic behaviour of complexes **1–4**, we performed DFT calculations to estimate their magnitude through the shortest X···X contacts

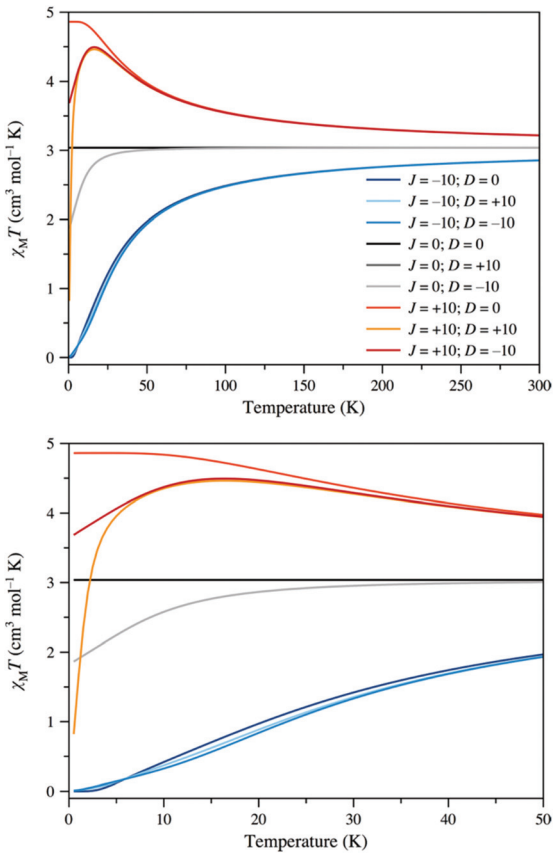

Fig. 6 Theoretical thermal dependence of the $\chi_M T$ product for a Re_2^{IV} model complex as a function of different J and D values with g = 1.8. The lower panel highlights the regime in the temperature range 0–50 K.

(X = Cl or Br). A summary of these results is given in Table 1. It is clear from this table that the intermolecular exchange interactions are very small for **2** and **4** and negligible for **1** and **3**.

In a spin-polarization mechanism the number of intervening atoms should dictate the nature of the magnetic exchange. Thus odd and even numbers of atoms favour ferromagnetic (F) and antiferromagnetic (AF) interactions, respectively. Hence, while the pyrazine ligand in **1** and **2** should mediate AF coupling, the pyrimidine and triazine ligands in **3** and **4** should promote F interactions. DFT calculations, summarised in Table 2, support this hypothesis. The spin density maps obtained for the broken-symmetry function corresponding to the spin ground states of **1–4** are shown in Fig. 7. The alternation between the spin densities on contiguous atoms in the

Table 1 Shortest X···X intermolecular contacts between neighbouring complex dianions in **1–4** together with their corresponding calculated magnetic coupling constants (J)

Compound	d(X···X)/Å	J/cm^{-1}
1	4.695	−0.04
2	3.520	−0.23
3	4.705	−0.007
4	3.430	−0.55

Table 2 Magnetic coupling constants (J) in the Re_2^{IV} moieties calculated for **1–4** and for the simplified models described in the text, each containing just one of the possible exchange pathways (diazine, Model A; Br, Model B). Two results are supplied for **3** because of the presence of two crystallographically independent Re_2^{IV} molecules in the structure

System	J/cm^{-1}	J/cm^{-1}, Model A	J/cm^{-1}, Model B
1	−10.1		
2	−8.9		
3a	+2.7	+5.4	−0.4
3b	+1.9	+4.6	−0.6
4	+3.0	+4.4	−0.1

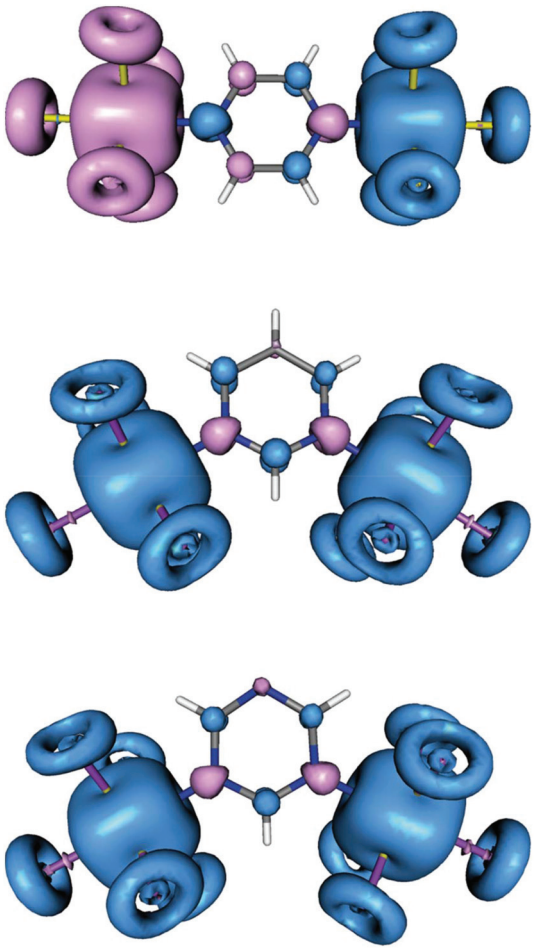

Fig. 7 Spin density plots for the ground spin states in (representative) **1** (top), **3** (middle) and **4** (bottom). The isodensity surfaces correspond to a cut-off value of 0.002 e bohr^{-3}. Blue and magenta isosurfaces represent positive and negative regions of spin density, respectively.

π-pathway is clear, and is suggestive of the presence of an operative McConnell mechanism.

However, the position of the two adjacent bromide ions in **3** and **4** (Fig. 1c and d; Fig. 7, middle and bottom) results in a short intramolecular Br···Br contact (~4 Å) that could potentially offer an alternative (dipolar) pathway for magnetic exchange. In order to check this, two models were built to esti-

mate the contribution through bonds and space, aimed at determining unambiguously the mechanism that governs the magnetic coupling in **3** and **4** (Table 2). The bromide ions mediating the alternative pathway in Model A were removed, and the diazine ligands in Model B were removed. Such a semi-quantitative approach, based on a change in the coordination sphere, is valid here because the electronic configuration of three unpaired electrons in the t_{2g} orbitals for the Re^{IV} ions is maintained. The results show that only the diazine ligand is able to mediate ferromagnetic exchange.

Re^{IV} ions present large zero-field splitting (zfs), which results in the separation of the M_S states of the $S = 3/2$ spin state. The magnitude of the parameters defining this physical phenomenon (D and E, the axial and rhombic components) directly depends on the molecular geometry and on the nature of the ligands that make up the coordination sphere of the metal ion. This can lead to additional complications in the interpretation of experimental and theoretical data. Fortunately, theoretical post-Hartree–Fock methods based on a Complete Active Space (CAS), that are more advanced than N-Electron Valence State Perturbation Theory (NEVPT2), have been previously used to a satisfactory level for the evaluation of the parameters that govern the zfs in Re^{IV} complexes. Theoretical results calculated on mononuclear models are given in Table 3. These models were built by (a) removing one of the Re^{IV} ions together with its ligands, or (b) by replacing the Re^{IV} ion with a Pb^{IV} ion. In general, the sign and magni-

Table 3 Axial (D) and rhombic (as E/D ratio) zfs parameters calculated on the models described in the text. The Re(i) notation is used to describe the mononuclear models and the i index indicates the number of Re centres. RePb and PbRe labels are used to describe the dinuclear model equivalent to Re(1) and Re(2), respectively. The identifications *a* and *b* are used to differentiate between the different Re_2 units that coexist in **3**

		CAS		NEVPT2	
Compound	Model	D/cm^{-1}	E/D	D/cm^{-1}	E/D
1	Re(1)	−10.0	0.173	−10.0	0.215
	RePb	−10.3	0.176	−10.2	0.208
	Re(2)	−5.1	0.082	−4.1	0.205
	PbRe	−5.6	0.066	−4.5	0.181
2	Re(1)	−6.6	0.247	−6.3	0.292
	RePb	−7.7	0.207	−7.3	0.260
3	Re(1)_*a*	−7.5	0.183	−9.4	0.110
	RePb_*a*	−7.7	0.311	−9.3	0.243
	Re(2)_*a*	−15.7	0.201	−17.4	0.184
	PbRe_*a*	−18.0	0.148	−19.9	0.135
	Re(1)_*b*	−11.4	0.192	−13.1	0.164
	RePb_*b*	−11.0	0.280	−12.7	0.247
	Re(2)_*b*	−8.7	0.138	−9.6	0.165
	PbRe_*b*	−11.5	0.170	−12.6	0.191
4	Re(1)	−10.6	0.184	−11.6	0.193
	RePb	−12.6	0.184	−13.8	0.199

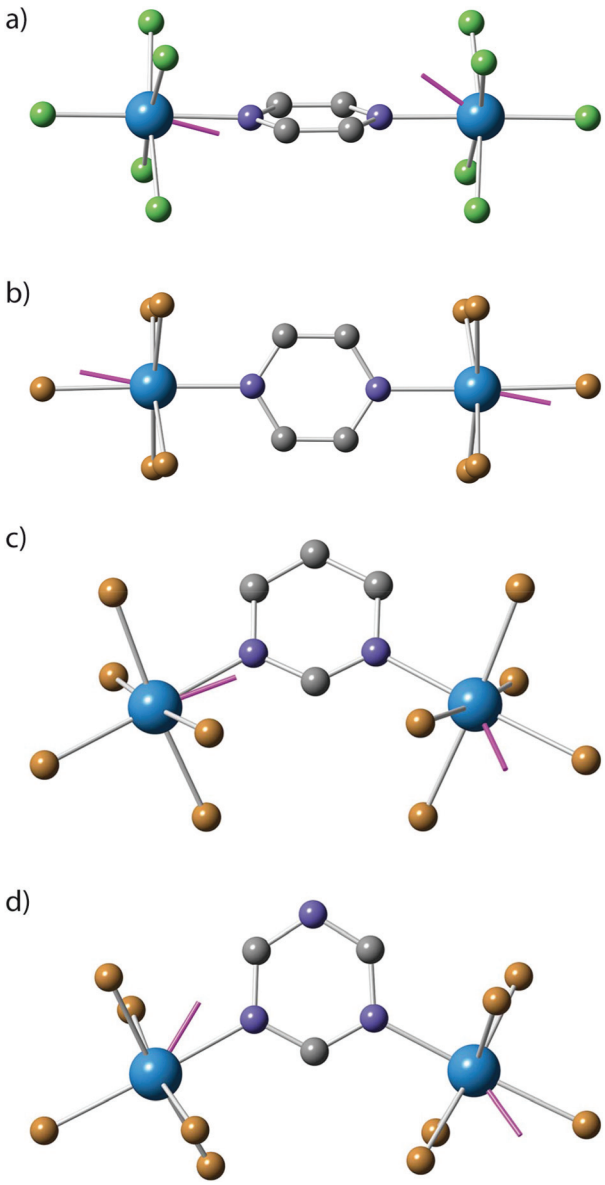

Fig. 8 Relative orientation of the z-axes (magenta sticks) of the local zfs tensors of Re^{IV} ions in **1** (a), **2** (b), **3a** (c) and **4** (d) obtained by CAS calculations. Hydrogen atoms are omitted for clarity. Colour code: cyan (rhenium), blue (nitrogen), green (chlorine), brown (bromine) and grey (carbon).

Table 4 Best-fit parameters obtained with spin Hamiltonian (1) and the thermal dependence of $\chi_M T$ for **1–4**. F is the agreement factor defined as $F = \sum[(\chi_M T)_{exp}{}^2 - (\chi_M T)_{calc}{}^2]/\sum(\chi_M T)_{exp}{}^2$. Compound **4** required the inclusion of a small intermolecular interaction, θ

Compound	g(Re)	D(Re)/cm^{-1}	J/cm^{-1}	θ/K	$F \times 10^5$
1	1.819 ± 0.007	−8.9 ± 0.6	−20.22 ± 0.15	—	6.8
2	1.883 ± 0.004	−7.4 ± 0.3	−19.08 ± 0.08	—	3.0
3	1.855 ± 0.003	+10.90 ± 0.16	0.77 ± 0.03	—	0.4
4	1.87 ± 0.04	+21 ± 3	+6.7 ± 1.2	−0.14 ± 0.08	10

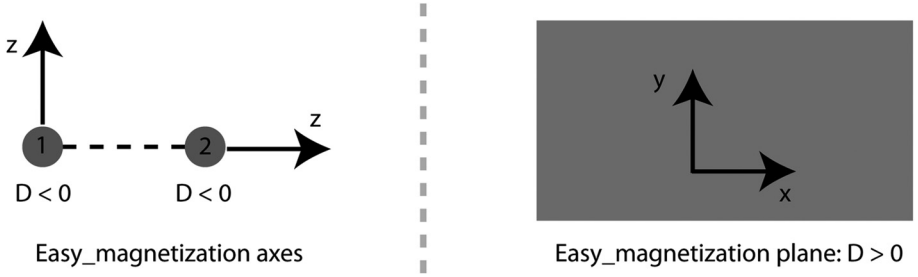

Fig. 9 Scheme to visualize how two perpendicular easy-magnetization axes turn into an easy-magnetization plane.

tude of the calculated values of D fall within a small range, and only small discrepancies in the E values are observed. Most cases point towards negative D values, *i.e.* states with higher $|M_S|$ values are stabilised, and they are in the range −5 to −15 cm^{-1}, the majority being placed around −10 cm^{-1}. This variation highlights the strong dependence of D on the small changes in geometry. Replacing the chloride ligands in **1** by bromide ions in **2–4** also has an effect on $|D|$. The impact is even observed in **3**, where the same compound exists in two non-equivalent dinuclear units (**3a** and **3b**), and where there is no inversion symmetry (**1** and **3**). Calculations were also performed on models where one of the Re^{IV} ions has been replaced by a Pb^{IV} ion, in order to minimize other electronic effects. The results show that both Re^{IV} and Re^{IV}–Pb^{IV} models provide the same (or very close) D values in all cases (Table 3).

With the theoretical study in mind, we modelled the experimental magnetic data with spin-Hamiltonian (1) in which the only variable parameters were the g-factor, J and D. Least-squares best-fit parameters obtained for **1–4** are shown as solid lines in Fig. 2–5, and are summarized in Table 4. The results agree well with those proposed in the theoretical study, although the magnitude of the experimental magnetic coupling is somewhat greater than those calculated from theory. Despite a negative D value being expected for **4**, the sharp drop in $\chi_M T$ at low temperature can be reproduced only with positive values. This discrepancy is related to the simplistic nature of our model. In a model that considers collinear local zfs tensors, a positive D value for the ferromagnetic $S = 3$ ground state can only be achieved from positive local D values. This approach causes no problem in **1** and **2** because their local zfs tensors are parallel or near parallel (Fig. 8). However, this is not the case in **3** and **4** where the z-axes of the local zfs tensors are almost perpendicular (Fig. 8). In the ferromagnetic state, they therefore conform to an easy-magnetization plane, *i.e.*, the D parameter takes a positive value (Fig. 9). A more detailed/rigorous analysis of the magnetic data would demand the inclusion of the relative orientation of the local zfs tensors, but it would likely over-parameterize our model.

Conclusions

A family of dirhenium(IV) complexes has been prepared by reaction between $[ReX_6]^{2-}$ (X = Cl and Br) building blocks and the bidentate N-donors pyz (**1** and **2**), pym (**3**) and triz (**4**). Coupled variable-temperature magnetic measurements and theoretical calculations on the structurally characterised compounds established that a spin polarization mechanism governs the intramolecular magnetic exchange interactions in all four complexes. These are antiferromagnetic for an even number of intervening atoms in the exchange pathway, *i.e.* for the bridging pyz molecule in **1** and **2**, and ferromagnetic for an odd number of intervening atoms in the exchange pathway, *i.e.* the bridging pyim (**3**) and triz ligands (**4**).

Conflicts of interest

There are no conflicts to declare.

Acknowledgements

We thank the EPSRC (EKB), the Spanish Ministerio de Economía y Competitividad (MINECO) (Projects CTQ2016-75068P and CTQ2016-75671P and Unidad de Excelencia María de Maetzu MDM-2015-0538) and the Generalitat Valencina (Project PROMETEO/2014/070) for financial support. JML thanks the MINECO for a Ramón y Cajal grant.

References

1 H. M. McConnell, *J. Chem. Phys.*, 1963, **39**, 1910.
2 A. Raja, S. Rajca and S. R. Desai, *J. Am. Chem. Soc.*, 1995, **117**, 806.
3 A. Rajca and S. Utamapanya, *J. Am. Chem. Soc.*, 1993, **115**, 10688.
4 A. Rajca, *J. Am. Chem. Soc.*, 1990, **112**, 5890.
5 H. Iwamura and N. Koga, *Acc. Chem. Res.*, 1993, **26**, 346.
6 D. A. Dougherty, *Acc. Chem. Res.*, 1991, **24**, 88.
7 (*a*) A. Rajca, *Chem. Rev.*, 1994, **94**, 871; (*b*) A. R. Paital, T. Mitra, D. Ray, W. T. Wong, J. Ribas-Ariño, J. J. Novoa, J. Ribas and G. Aromí, *Chem. Commun.*, 2005, 5172; (*c*) A. R. Painal, A. Q. Wu, G. Cong, G. Aromí, J. Ribas-Ariño and D. Ray, *Inorg. Chem.*, 2007, **46**, 2947.
8 D. R. Corbin, L. C. Francesconi, D. N. Hendrikson and G. D. Stucky, *Inorg. Chem.*, 1979, **18**, 3069.

9 L. C. Francesconi, D. R. Corbin, D. N. Hendrickson and G. D. Stucky, *Inorg. Chem.*, 1979, **18**, 3074.
10 K. Inoue and H. Iwamura, *J. Am. Chem. Soc.*, 1994, **116**, 3173.
11 M. Kitano, N. Koga and H. Iwamura, *J. Chem. Soc., Chem. Commun.*, 1994, 447.
12 T. Ishida, S.-I. Mitsubori, T. Nogami and H. Iwamura, *Mol. Cryst. Liq. Cryst.*, 1993, **233**, 345.
13 S. L. W. McWhinnie, C. J. Jones, J. A. McCleverty, D. Collison and F. E. Mabbs, *J. Chem. Soc., Chem. Commun.*, 1990, 940.
14 A. Das, J. P. McCleverty, J. A. N. Badiola and M. D. Ward, *J. Chem. Soc., Dalton Trans.*, 1993, 681.
15 A. Das, J. C. Jeffery, J. P. Maher, J. A. McCleverty, E. Schatz, M. D. Ward and G. Wollermann, *Inorg. Chem.*, 1993, **32**, 2145.
16 A. J. Amoroso, A. M. W. Cargill Thompson, J. P. Maher, J. A. McCleverty and M. D. Ward, *Inorg. Chem.*, 1995, **34**, 4828.
17 A. M. W. Cargill Thompson, D. Gatteschi, J. A. McCleverty, J. A. Navas, E. Rentschler and M. D. Ward, *Inorg. Chem.*, 1996, **35**, 2701.
18 V. Â. Ung, A. M. W. Cargill Thompson, D. A. Bardwell, D. Gatteschi, J. C. Jeffery, J. A. McCleverty, F. Totti and M. D. Ward, *Inorg. Chem.*, 1997, **36**, 3447.
19 S. Bayly, J. A. McCleverty, M. D. Ward, D. Gatteschi and F. Totti, *Inorg. Chem.*, 2000, **39**, 1288.
20 F. Lloret, G. De Munno, M. Julve, J. Cano, R. Ruiz and A. Caneschi, *Angew. Chem., Int. Ed.*, 1998, **37**, 135.
21 I. Fernández, R. Ruiz, J. Faus, M. Julve, F. Lloret, J. Cano, X. Ottenwaelder, Y. Journaux and M. Carmen Muñoz, *Angew. Chem., Int. Ed.*, 2001, **40**, 3039.
22 E. Pardo, J. Faus, M. Julve, F. Lloret, M. Carmen Muñoz, J. Cano, X. Ottenwaelder, Y. Journaux, R. Carrasco, G. Blay, I. Fernández and R. Ruiz-García, *J. Am. Chem. Soc.*, 2003, **125**, 10770.
23 E. Pardo, R. Carrasco, R. Ruiz-García, M. Julve, F. Lloret, M. Carmen Muñoz, Y. Journaux, E. Ruiz and J. Cano, *J. Am. Chem. Soc.*, 2008, **130**, 576.
24 M. Castellano, R. Ruiz-García, J. Cano, J. Ferrando-Soria, E. Pardo, F. R. Fortea-Pérez, S.-E. Stiriba, M. Julve and F. Lloret, *Acc. Chem. Res.*, 2015, **48**, 510.
25 M. Castellano, R. Ruiz-García, J. Cano, J. Ferrando-Soria, E. Pardo, F. R. Fortea-Pérez, S.-E. Stiriba, W. P. Barros, H. O. Stumpf, L. Cañadillas-Delgado, J. Pasán, C. Ruiz-Pérez, G. de Munno, D. Armentano, Y. Journaux, F. Lloret and M. Julve, *Coord. Chem. Rev.*, 2015, **303**, 110.
26 J. Cano, F. Lloret and M. Julve, *Dalton Trans.*, 2016, **45**, 16700.
27 R. Chiozzone, R. González, C. Kremer, G. De Munno, J. Cano, F. Lloret, M. Julve and J. Faus, *Inorg. Chem.*, 1999, **38**, 4745.
28 J. Kleinberg, *Inorg. Synth*, McGraw-Hill, 1963.
29 G. A. Bain and J. F. Berry, *J. Chem. Educ.*, 2008, **85**, 532.
30 L. J. Bourhis, O. V. Dolomanov, R. J. Gildea, J. A. K. Howard and H. Puschmann, *Acta Crystallogr., Sect. A: Fundam. Crystallogr.*, 2015, **71**, 59.
31 G. Sheldrick, *Acta Crystallogr., Sect. A: Fundam. Crystallogr.*, 2008, **64**, 112.
32 O. V. Dolomanov, L. J. Bourhis, R. J. Gildea, J. A. K. Howard and H. Puschmann, *J. Appl. Crystallogr.*, 2009, **42**, 339.
33 M. J. Frisch, *Gaussian 09 (Revision C.01)*, Gaussian, Inc., Wallingford, CT, 2009.
34 A. D. Becke, *Phys. Rev. A*, 1988, **38**, 3098.
35 A. D. Becke, *J. Chem. Phys.*, 1993, **98**, 5648.
36 C. Lee, W. Yang and R. G. Parr, *Phys. Rev. B: Condens. Matter*, 1988, **37**, 785.
37 T. Yania, D. P. Tew and N. C. Handy, *Chem. Phys. Lett.*, 2004, **393**, 51; A. Schäfer, H. Horn and R. Ahlrichs, *J. Chem. Phys.*, 1992, **97**, 2571.
38 P. J. Hay and W. R. Wadt, *J. Chem. Phys.*, 1985, **82**, 270.
39 W. R. Wadt and P. J. Hay, *J. Chem. Phys.*, 1985, **82**, 284.
40 P. J. Hay and W. R. Wadt, *J. Chem. Phys.*, 1985, **82**, 299.
41 A. Schäfer, C. Huber and R. Ahlrichs, *J. Chem. Phys.*, 1994, **100**, 5829.
42 M. Douglas and N. M. Kroll, *Ann. Phys.*, 1974, **82**, 89.
43 A. B. Hess, *Phys. Rev. A*, 1985, **32**, 756.
44 E. Ruiz, J. Cano, S. Alvarez and P. Alemany, *J. Comput. Chem.*, 1999, **20**, 1391.
45 J. Tomasi, B. Mennucci and E. Cancès, *J. Mol. Struct.*, 1999, **464**, 211.
46 F. Neese, The ORCA program system, *WIREs Comput. Mol. Sci.*, 2012, **2**, 73.
47 C. Chang, M. Pelissier and Ph. Durand, *Phys. Scr.*, 1986, **34**, 394.
48 K. Eichkorn, O. Treutler, H. Ohm, M. Haser and R. Ahlrichs, *Chem. Phys. Lett.*, 1995, **240**, 283.
49 K. Eichkorn, O. Treutler, H. Ohm, M. Haser and R. Ahlrichs, *Chem. Phys. Lett.*, 1995, **242**, 652.
50 K. Eichkorn, F. Weigend, O. Treutler and R. Ahlrichs, *Theor. Chem. Acc.*, 1997, **97**, 119.
51 C. Angeli, R. Cimiraglia, S. Evangelisti, T. Leininger and J.-P. Malrieu, *J. Chem. Phys.*, 2001, **114**, 10252.
52 C. Angeli, R. Cimiraglia and J.-P. Malrieu, *Chem. Phys. Lett.*, 2001, **350**, 297.
53 C. Angeli, R. Cimiraglia and J.-P. Malrieu, *J. Chem. Phys.*, 2002, **117**, 9138.
54 J. Martinez-Lillo, D. Armentano, N. Marino, L. Arizaga, R. Chiozzone, R. Gonzalez, C. Kremer, J. Cano and J. Faus, *Dalton Trans.*, 2008, 4585.
55 G. Chen, W.-L. Man, S.-M. Yiu, T.-W. Wong, L. Szeto, W.-T. Wong and T.-C. Lau, *Dalton Trans.*, 2011, **40**, 1938.
56 A. Skarżyńska and M. Siczek, *Polyhedron*, 2008, **27**, 1930.
57 A. Cuevas, C. Kremer, M. Hummert, H. Schumann, F. Lloret, M. Julve and J. Faus, *Dalton Trans.*, 2007, 342.
58 N. Nédélec and F. D. Rochon, *Inorg. Chem.*, 2001, **40**, 5236.
59 J. T. Maeyer, T. J. Johnson, A. K. Smith, B. D. Borne, R. D. Pike, W. T. Pennington, M. Krawiec and A. L. Rheingold, *Polyhedron*, 2003, **22**, 419.
60 (*a*) J. Martínez-Lillo, J. Faus, F. Lloret and M. Julve, *Coord. Chem. Rev.*, 2015, **289–290**, 215–237; (*b*) S. Kumar Singh and G. Rajaraman, *Nat. Commun.*, 2016, **7**, 10669.